A Novel N-Methyltransferase in Arabidopsis Appears to Feed a Conserved Pathway for Nicotinate Detoxification among Land Plants and Is Associated with Lignin Biosynthesis[1][OPEN]

Wei Li,[a,2] Fengxia Zhang,[a,2] Ranran Wu,[a,2] Lijia Jia,[b] Guosheng Li,[a,c] Yalong Guo,[d] Cuimin Liu,[b] and Guodong Wang[a,3]

[a]State Key Laboratory of Plant Genomics and National Center for Plant Gene Research, Institute of Genetics and Developmental Biology, Chinese Academy of Sciences, Beijing 100101, China
[b]State Key Laboratory of Plant Cell and Chromosome Engineering and Center for Molecular Agrobiology, Institute of Genetics and Developmental Biology, Chinese Academy of Sciences, Beijing 100101, China
[c]University of the Chinese Academy of Sciences, Beijing 100039, China
[d]State Key Laboratory of Systematic and Evolutionary Botany, Institute of Botany, Chinese Academy of Sciences, Beijing 100093, China

ORCID IDs: 0000-0002-9325-1882 (R.W.); 0000-0002-8994-8011 (L.J.); 0000-0001-5938-2750 (G.L.); 0000-0003-4982-4804 (C.L.); 0000-0001-9917-0656 (G.W.).

The Preiss-Handler pathway, which salvages nicotinate (NA) for NAD synthesis, is an indispensable biochemical pathway in land plants. Various NA conjugations (mainly methylation and glycosylation) have been detected and have long been proposed for NA detoxification in plants. Previously, we demonstrated that NA *O*-glucosylation functions as a mobilizable storage form for NAD biosynthesis in the Brassicaceae. However, little is known about the functions of other NA conjugations in plants. In this study, we first found that *N*-methylnicotinate is a ubiquitous NA conjugation in land plants. Furthermore, we functionally identified a novel methyltransferase (At3g53140; NANMT), which is mainly responsible for *N*-methylnicotinate formation, from Arabidopsis (*Arabidopsis thaliana*). We also established that trigonelline is a detoxification form of endogenous NA in plants. Combined phylogenetic analysis and enzymatic assays revealed that NA *N*-methylation activity was likely derived from the duplication and subfunctionalization of an ancestral caffeic acid *O*-methyltransferase (*COMT*) gene in the course of land plant evolution. COMT enzymes, which function in *S*-lignin biosynthesis, also have weak NANMT activity. Our data suggest that NA detoxification conferred by NANMT and COMT might have facilitated the retention of the Preiss-Handler pathway in land plants.

NAD is a ubiquitous coenzyme that serves as an electron carrier in hundreds of redox reactions. Multiple redox reactions related to core energy metabolism are NAD dependent, including reactions in glycolysis, the Krebs cycle, and the Calvin cycle. Common redox reactions that use NAD as an electron carrier do not generally lead to the net consumption of NAD in cells. Several types of NAD-consuming enzymes, which are conserved across living organisms, have been functionally identified. The physiological importance of such enzymes has rekindled interest in NAD metabolism generally, and NAD turnover and its implications in vivo have become active areas of research (Noctor et al., 2006; De Block and Van Lijsebettens, 2011). It is now known that NAD can be biosynthesized in plants via both a de novo pathway starting from Asp and by the Preiss-Handler salvage pathway (Katoh et al., 2006; Noctor et al., 2006; Wang and Pichersky, 2007). The Preiss-Handler pathway in land plants, as in most bacteria, starts with nicotinate (NA), which is generated from nicotinamide (NAM) by nicotinamidase (NIC), catalyzed sequentially by nicotinate phosphoribosyltransferase (NaPRT), nicotinate mononucleotide adenylyltransferase (NaMNAT), and NAD synthase (NADS; Fig. 1; Preiss and Handler, 1958a, 1958b; Wang and Pichersky, 2007; Li et al., 2015b). Most animals and the green alga *Chlamydomonas reinhardtii*, however, use a

[1] This work was supported by the National Program on Key Basic Research Projects (973 Program grant no. 2013CB127000), the National Natural Sciences Foundation of China (grant no. 31270336), and the State Key Laboratory of Plant Genomics of China (grant no. 2014b0227-05) to G.W.

[2] These authors contributed equally to the article.

[3] Address correspondence to gdwang@genetics.ac.cn.

The author responsible for distribution of materials integral to the findings presented in this article in accordance with the policy described in the Instructions for Authors (www.plantphysiol.org) is: Guodong Wang (gdwang@genetics.ac.cn).

G.W. conceived and designed the research; W.L., R.W., and G.L. performed the research; F.Z., Y.G., and L.J. contributed new reagents/analytic tools; G.W., W.L., F.Z., and R.W. analyzed data; G.W., W.L., and C.L. wrote the article.

[OPEN] Articles can be viewed without a subscription.

www.plantphysiol.org/cgi/doi/10.1104/pp.17.00259

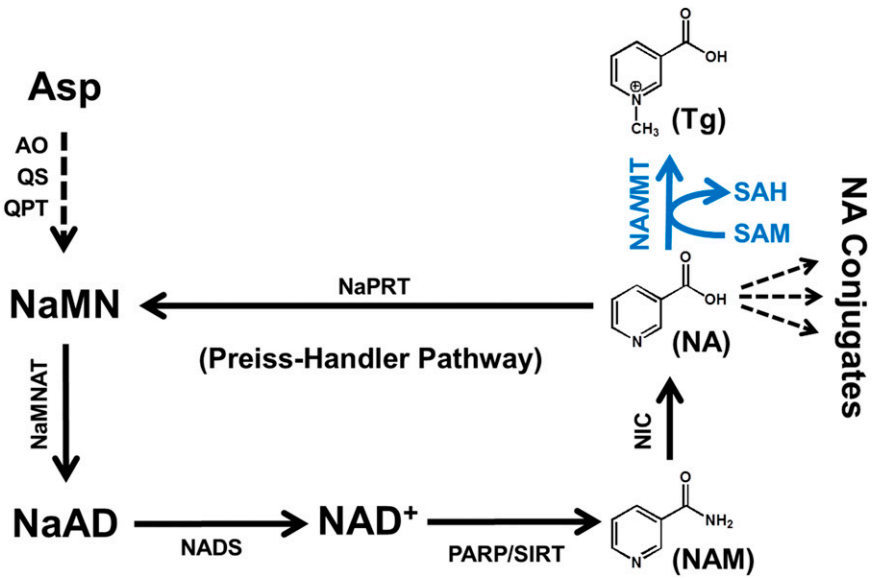

Figure 1. Tg biosynthesis and NAD metabolism in land plants. The step catalyzed by NA*N*MT is indicated in blue. AO, Asp oxidase; NaAD, nicotinate adenine dinucleotide; NaMN, nicotinate mononucleotide; PARP, poly(ADP-ribose) polymerase; QPT, quinolinate phosphoribosyltransferase; QS, quinolinate synthase; SAH, *S*-adenosylhomocysterin; SAM, *S*-adenosylmethionine; SIRT, sirtuins (NAD-dependent protein deacetylases).

two-reaction pathway in which NAM is converted directly to nicotinamide mononucleotide (NMN) by nicotinamide phosphoribosyltransferase, whereupon NMN is then converted to NAD by nicotinamide mononucleotide adenylyltransferase. This two-step pathway does not include the production of NA, and no close homologs of the Preiss-Handler pathway genes *NIC* or *NaPRT* have been identified in the genomes of green algae or animals (Rongvaux et al., 2003; Noctor et al., 2006; Li et al., 2015b). The overaccumulation of NA has been demonstrated to be toxic to plant cells (Zheng et al., 2005; Wang and Pichersky, 2007; Li et al., 2015b). We previously proposed that plants evolved various strategies to deal with NA toxicity based on the fact that various conjugates of NA (glycosylation or methylation at the *N*-position or carboxyl group of NA) have been detected in plants. We further demonstrated that NA *O*-glucosylation functions to detoxify NA and that this process is likely restricted to the Brassicaceae (Li et al., 2015b).

Trigonelline (Tg; *N*-methylnicotinate), an alkaloid that was named after its isolation from the seeds of *Trigonella foenum-graecum*, has been found in a wide range of plant species from ferns to flowering plants (Matsui et al., 2007; Ashihara et al., 2012; Zhou et al., 2012; Li et al., 2015b). Tg also is known to be beneficial to human health by affecting Glc metabolism and lowers the risk of type 2 diabetes, and it accounts for approximately 1% of the dry matter in coffee (*Coffea arabica*) beans (Allred et al., 2009; van Dijk et al., 2009). The potential use of Tg in other therapies was reviewed recently (Zhou et al., 2012). Tg is synthesized from NA, the intermediate metabolite in the Preiss-Handler pathway. However, little is known about its physiological functions in planta. Tg came to the attention of plant biologists because it appeared to function as a plant hormone and was proposed to have a role as a cell cycle regulator in roots and shoot meristems (Evans et al., 1979). Subsequently, multiple studies established that Tg likely functions as a plant growth regulator in diverse processes such as nodulation, abiotic stress responses, DNA methylation, and nyctinasty (Minorsky, 2002). However, such ideas lacked supporting evidence at the genetic and molecular levels because no gene for a Tg synthase had been identified. A nicotinate *N*-methyltransferase (NA*N*MT) protein was partially purified from heterotrophic cell suspension cultures of soybean (*Glycine max*) and biochemical studies established that NA*N*MT, like other plant natural product methyltransferases, uses SAM as a methyl donor (Upmeier et al., 1988). However, no *NANMT* cDNA sequence has been cloned from soybean to date. Recently, two *NANMT* cDNAs (named CTgS1 and CTgS2, which belong to the SABATH methyltransferase family [also referred to as motif B′ methyltransferase]) were functionally identified in coffee (Mizuno et al., 2014). We previously screened all 24 Arabidopsis (*Arabidopsis thaliana*) SABATH proteins for catalytic activity with 59 potential substrates, including NA, and no NA*N*MT activity was detected (Yang et al., 2006a, 2006b). One AtSABATH protein encoded by *At5g04370* methylated NA at the carboxyl group rather than the *N*-position to form NA methyl ester (Yang et al., 2006a). These studies suggested that another type of methyltransferase was recruited for Tg production in Arabidopsis, illustrating a case of convergent evolution in plant specialized metabolism (Pichersky and Lewinsohn, 2011).

Since the first structure of a plant natural product methyltransferase (chalcone *O*-methyltransferase) was reported in 2001, the structures of several plant methyltransferases with diverse methyl acceptor products have been elucidated (Zubieta et al., 2001; Gang et al., 2002; McCarthy and McCarthy, 2007; Louie et al., 2010). These studies revealed that all plant SAM-dependent methyltransferases share a highly conserved structure (especially the SAM-binding domain), although they have little sequence identity (Martin and McMillan, 2002; Liscombe et al., 2012). This structural property of plant methyltransferases and the relatively large size of methyltransferase gene families in plants (e.g. 478 genes

were found in a search of the Arabidopsis genome annotation database using the search term methyltransferase; www.arabidopsis.org) make it very difficult to predictively determine the particular substrate(s) of a given methyltransferase. In mammals, the nicotinamide *N*-methyltransferase (hNNMT; GenBank accession no. U08021) has been characterized biochemically and structurally (Aksoy et al., 1994; Peng et al., 2011). Although the chemical structure of NA is similar to that of NAM (Fig. 1), no *hNNMT* homologs (greater than 20% identity at the protein level) could be found in any plant genome.

In this study, using gene-enzyme correlation analysis (Li et al., 2015b), we identified a novel methyltransferase (not a SABATH methyltransferase) that is responsible mainly for Tg production in Arabidopsis. We demonstrate that the in planta physiological functions of Tg include the detoxification of endogenous NA and involvement in NAD homeostasis. Phylogenetic analysis and biochemical characterization of related methyltransferase proteins from 10 plant species, selected based on their positions at important evolutionary nodes, clearly indicated that the conserved *NANMT* proteins probably evolved from plant caffeic acid *O*-methyltransferases (COMTs), which also have weak NANMT activity across the land plants. Based on our results, we propose that NA detoxification conferred by NANMT and COMT facilitated the retention of the Preiss-Handler pathway in land plants. Our discovery also paves the way for investigations of other physiological functions of Tg in land plants.

RESULTS

Tg Is Detected in Basal Land Plants

Although Tg has been detected in a wide range of vascular plants (Ashihara et al., 2012; Li et al., 2015b), our knowledge of the distribution of Tg in basal land plants is still lacking. Thus, we used two methods to test

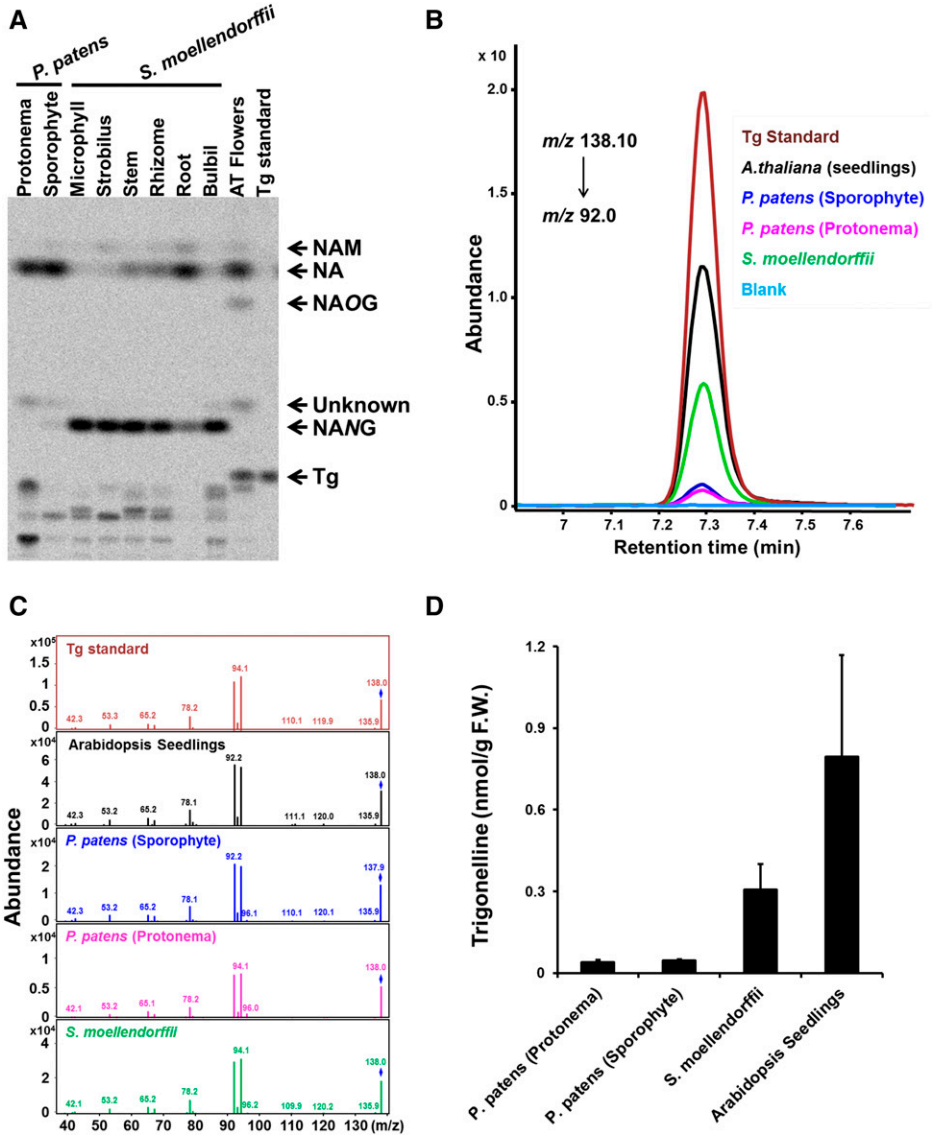

Figure 2. Tg in *S. moellendorffii* and *P. patens*. A, ^{14}C-Labeled NAM feeding of different tissues of *S. moellendorffii* and *P. patens* (both protonema and sporophyte stages). Tissues were incubated with 10 μM [^{14}C]NAM for 2 h. B, LC-QQQ-MS analysis (multiple reaction monitoring; mass-to-charge ratio 138.1 to 92) of an authentic Tg reference standard, endogenous Tg from Arabidopsis seedlings (2 weeks old), and endogenous Tg from *S. moellendorffii* and *P. patens* (both protonema and sporophyte stages). C, Full-scan mass spectra of the Tg standard, endogenous Tg from Arabidopsis seedlings (2 weeks old), and endogenous Tg from *S. moellendorffii* and *P. patens* (both protonema and sporophyte stages). D, Tg content in Arabidopsis (2-week-old seedlings), *S. moellendorffii*, and *P. patens*. Data represent means ± SD (n = 3). F.W., Fresh weight.

whether Tg is produced in basal land plants and the green alga *C. reinhardtii* strain cc400. We fed different organs of *Physcomitrella patens* (Bryophytes) and *Selaginella moellendorffii* (Pteridophytes) with 10 μM [^{14}C]NAM and assayed for Tg synthase activity in planta (Supplemental Fig. S1). We also used liquid chromatography triple quadrupole mass spectrometry (LC-QQQ-MS) to analyze the endogenous Tg content in *S. moellendorffii* and *P. patens* at both the protonema and sporophyte stages. Although no clear signal for [^{14}C]Tg was detected in the [^{14}C]NAM feeding experiments (Fig. 2A), the LC-QQQ-MS analysis showed that endogenous Tg was clearly present in both *S. moellendorffii* (0.31 $\pm$ 0.094 nmol g^{-1} fresh weight; n = 3) and *P. patens* (0.039 $\pm$ 0.0093 nmol g^{-1} fresh weight in protonema material and 0.047 $\pm$ 0.0045 nmol g^{-1} fresh weight in sporophyte material; n = 3; Fig. 2, B–D). These results suggest that Tg is widely distributed in land plants.

Functional Characterization of *NANMT* from Arabidopsis

We previously profiled NA conjugates in seven different tissues of Arabidopsis and found that [^{14}C]Tg accumulates (reflecting NANMT activity) predominantly in inflorescence tissues but also is present in stems and siliques (see Fig. 1 in Li et al., 2015b). Here, we used the same strategy (gene-enzyme correlation analysis) to identify eight candidate genes (*At4g10440*, *At1g67990*, *At3g53140*, *At5g53810*, *At5g51130*, *At5g37170*, *At3g51070*, and *At1g04050*) from a total of 289 annotated methyltransferase probes ($P < 0.001$; Supplemental Data Set S1). Open reading frames were finally obtained for six candidate genes, and the protein encoded by *At3g53140* clearly had the *N*-methyltransferase activity with NA as a substrate (Fig. 3). Therefore, At3g53140 was designated as AtNANMT1. AtNANMT1 did not show any detectable activity with NAM in the same enzymatic assay. AtNANMT1 displayed similar levels of activity at pH values ranging from 5 to 8, and NANMT activity was not stimulated significantly by the presence of various metal ions (Supplemental Fig. S2). NANMT had an apparent K_m value of 38.7 $\pm$ 1.99 μM (n = 3) for NA, and its K_{cat} value was 3.52 $\pm$ 0.082 s^{-1} (n = 3; Table I).

To deepen our understanding of the in planta function of Tg, two types of transgenic plants were generated. First, two independent lines with T-DNA insertions in

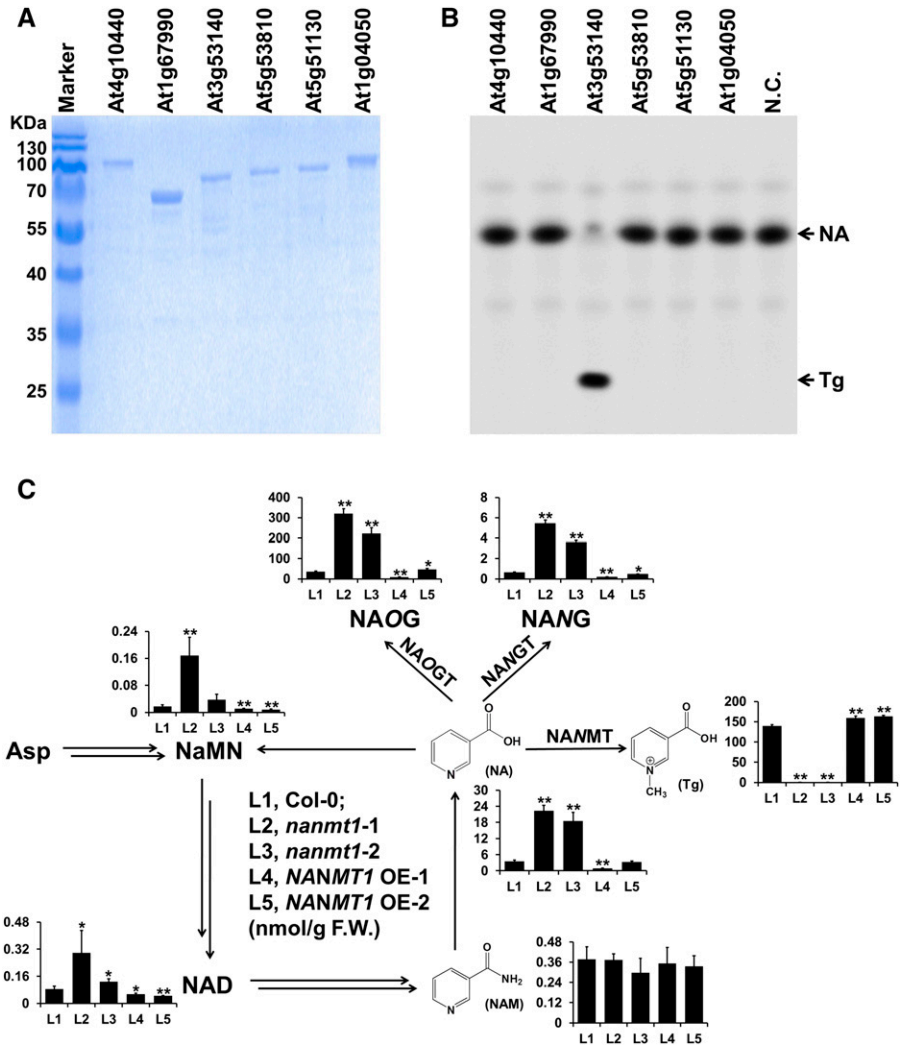

Figure 3. Functional characterization of *NANMT1* in Arabidopsis. A, SDS-PAGE analysis of six purified maltose-binding protein (MBP)-tagged NANMT candidate proteins. B, Radio-thin-layer chromatography (TLC) analysis of Tg produced by the purified recombinant NANMT candidate proteins using [^{14}C]NA and SAM as substrates. Only one protein (At3g53140) showed obvious NANMT activity. N.C., Negative control, in which no protein was added to the NANMT assay. C, Chemical characterization of the inflorescences of *AtNANMT1* transgenic plants. Bars show means $\pm$ SD (n = 4). Asterisks indicate significant differences from wild-type plants: *, $P < 0.05$ and **, $P < 0.01$ (two-tailed Student's t test). F.W., Fresh weight.

AtNANMT1 were isolated and characterized; no *NANMT1* transcripts could be detected in either mutant. Crude protein extracts were prepared from inflorescence tissue where *AtNANMT1* was highly expressed but did not show any NANMT activity (Supplemental Fig. S3, A–C). Therefore, these two null mutant alleles were designated as *nanmt1-1* (SALK_046243) and *nanmt1-2* (SALK_071460). Second, transgenic plants (Columbia background [Col-0]) expressing *AtNANMT1* under the control of the cauliflower mosaic virus 35S promoter were generated and characterized. Two independent lines (OE-1 and OE-2) with high NANMT activity in crude protein extracts from young seedlings were selected for further experiments (Supplemental Fig. S3, D and E).

Homozygous *nanmt1-1* and *nanmt1-2* lines showed marked reductions in Tg accumulation in inflorescence tissues, whereas the levels of NA, glucosylated NA (NAOG and NANG), NaMN, and NAD were increased significantly (Fig. 3C). As expected, relative to wild-type plants, the OE-1 and OE-2 lines had higher Tg content and lower NA, NAOG, NANG, NaMN, and NAD contents (Fig. 3C). Although the chemical profiles were altered dramatically, the expression patterns of genes involved in NAD biosynthesis and NA modification were largely unchanged in inflorescence tissues, with the exception of *NIC1*, whose expression increased by 2-fold in the OE-1 and OE-2 lines (Supplemental Fig. S4). Similar patterns of NA, Tg, NAOG, and NANG accumulation also were found in the developing seeds of all tested plants (Supplemental Fig. S5).

Quantitative PCR analysis verified that *AtNANMT1* was expressed at the highest level in inflorescence tissue, a finding consistent with the strong accumulation of Tg in inflorescences in the Tg profiling experiments (Fig. 4A). Analysis of plants expressing a Pro_{NANMT1}:*GUS* transgene further confirmed the inflorescence-specific expression pattern of *AtNANMT1*. *AtNANMT1* expression was especially strong in anthers, developing siliques, and developing seeds (Fig. 4B). The subcellular localization of the NANMT1:GFP fusion protein in protoplasts indicated that AtNANMT1 is a cytosolic protein (Fig. 4C).

Taken together, the results of these functional characterization experiments enable us to conclude that NANMT1 encoded by *At3g53140* is the enzyme responsible for Tg biosynthesis in Arabidopsis. It should be noted that low but detectable levels of Tg were found in *nanmt1* mutants (inflorescence tissue and developing seeds; Fig. 3C; Supplemental Fig. S5), suggesting that the loss of AtNANMT1 activity does not completely block the production of Tg in Arabidopsis.

NANMT Is Involved in NA Detoxification in Arabidopsis

None of the *AtNANMT1* transgenic plants showed obvious phenotypic abnormalities, even in the inflorescence tissue where *NANMT1* was most highly expressed (Supplemental Fig. S6). However, we did find that seedlings of the OE-1 (6.75 ± 0.4 cm in root length; $n = 4$) and OE-2 (7.3 ± 0.68 cm; $n = 4$) lines grew much faster (as measured by root length) than wild-type (5.38 ± 0.4 cm; $n = 4$) or *nanmt1* (5.63 ± 0.69 cm for *nanmt1-1* and 5.22 ± 0.52 cm for *nanmt1-2*; $n = 4$) plants when grown on one-half-strength Murashige and Skoog (1/2 MS) medium plates supplemented with 100 μM NA (Fig. 5, B and D). In contrast, Tg treatment did not inhibit the root growth of any of the tested lines, and no significant differences in

Table I. *Catalytic efficiency of plant NANMT enzymes*

All data obtained in this study are presented as means ± SD from triplicate independent assays. N/A, Not applicable.

Enzyme	Substrate	K_m	K_{cat}	K_{cat}/K_m
		μM	s^{-1}	$\mu M^{-1}\ s^{-1}$
AtNANMT1	NA[a]	38.70 ± 1.99	3.52 ± 0.082	0.091 ± 0.0063
	SAM[b]	52.13 ± 2.51	3.01 ± 0.060	0.058 ± 0.0017
Gm13G263200	NA[a]	55.86 ± 3.08	4.81 ± 0.086	0.086 ± 0.0038
	SAM[b]	69.20 ± 4.05	4.14 ± 0.091	0.060 ± 0.0027
Os02g57760	NA[a]	43.62 ± 0.91	2.25 ± 0.012	0.051 ± 0.0010
	SAM[b]	67.26 ± 4.06	2.07 ± 0.019	0.031 ± 0.0015
Aco_009_01073	NA[a]	67.90 ± 7.33	5.83 ± 0.11	0.086 ± 0.0078
	SAM[b]	69.83 ± 5.64	4.44 ± 0.14	0.064 ± 0.0032
PineTC169872	NA[a]	60.58 ± 1.66	4.97 ± 0.071	0.082 ± 0.0021
	SAM[b]	71.70 ± 9.90	3.94 ± 0.23	0.055 ± 0.0044
Sly10g085830	NA[a]	45.80 ± 1.42	2.37 ± 0.068	0.051 ± 0.0030
	SAM[b]	64.28 ± 7.67	1.92 ± 0.083	0.030 ± 0.0030
Tca1EG022341t1	NA[a]	37.19 ± 3.18	2.94 ± 0.052	0.079 ± 0.0071
	SAM[b]	40.57 ± 4.72	2.42 ± 0.090	0.060 ± 0.0065
Crude protein[c]	NA[a]	36.54 ± 3.41	N/A	N/A
	SAM[b]	66.37 ± 13.61	N/A	N/A

[a]Kinetic parameters for NA were determined with 500 μM SAM. [b]Kinetic parameters for SAM were determined with 200 μM NA. [c]The crude protein was prepared from inflorescences of 6-week-old Arabidopsis plants.

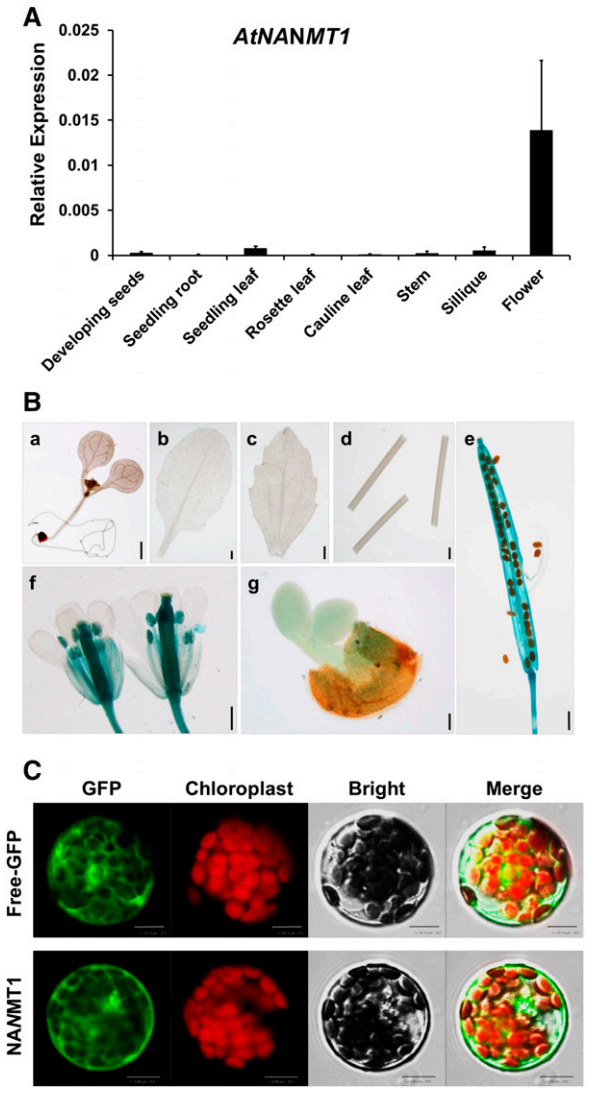

Figure 4. Spatial expression patterns and subcellular localization of *AtNANMT1* in Arabidopsis. A, Quantitative reverse transcription-PCR analysis of *AtNANMT1* expression in different tissues of Arabidopsis. Bars represent means ± SD (n = 3). B, Histochemical GUS staining of Pro_{NANMT1}:*GUS* transgenic plants. All samples were stained for 4 h. a, Ten-day-old seedling; b, rosette leaf; c, cauline leaf; d, stem; e, green silique (9–10 weeks old); f, flowers; g, developing seeds (from 9- to 10-week-old siliques). Bars = 1 mm. C, Subcellular localization of AtNANMT1 in Arabidopsis leaf mesophyll protoplasts. GFP fusion proteins were visualized by laser confocal microscopy. Chloroplasts are represented by red chlorophyll autofluorescence. Bars = 10 μm.

root length between wild-type or *nanmt1* plants were observed in this experiment (Fig. 5, C and D). Chemical analysis showed that the OE-1 and OE-2 seedlings accumulated lower levels of NA than wild-type and *nanmt1* seedlings under NA treatment. The endogenous NA level is negatively correlated with the root length of wild-type and *NANMT1* transgenic seedlings (Fig. 5, D and E). Given the toxic nature of NA, these results suggest that NA *N*-methylated NA is a detoxified form of endogenous NA in planta.

Previously, Shimizu and Mazzafera (2000) found that Tg was demethylated for NAD biosynthesis during the early stages of coffee seed germination. To determine the metabolic fate of Tg in Arabidopsis, we fed four Arabidopsis tissues (2-week-old seedlings, cauline leaves, inflorescences, and siliques) with purified [carboxyl-^{14}C]Tg for 20 h. However, only [^{14}C]Tg, and no [^{14}C]NAD or other labeled chemicals, was detected in this experiment (Supplemental Fig. S7). This result indicates that Tg cannot be reutilized for NAD biosynthesis, which is consistent with the results of labeling experiments in mung bean (*Vigna radiata*; Zheng et al., 2005).

Phylogenetic and Enzymatic Analyses of Plant NANMTs

To trace the evolutionary history of plant NANMTs, we constructed a phylogenetic tree of NANMT1 homologs and related methyltransferase proteins from all available plant genomes (Fig. 6A). Close homologs of AtNANMT1 could be found in all seed plants (greater than 40% protein identity to AtNANMT1). The closest homolog of AtNANMT1 in Arabidopsis is AtCOMT1 (encoded by *At5g54160*; 38% identity to AtNANMT1); this protein has been demonstrated to be responsible for *S*-lignin formation in planta (Goujon et al., 2003). The NANMT-like proteins and COMT-like proteins from seed plants are clearly separated. It is noteworthy that the related OMT proteins from the basal land plants (nine OMT proteins from *S. moellendorffii* and three OMT proteins from *P. patens*) have similar protein sequence identity (30%–40%) to both NANMT-like proteins and COMT-like proteins from seed plants. No close homologs of NANMT and COMT could be found in *C. reinhardtii* (less than 20% protein identity). Despite the fact that there are high levels of Tg accumulation in coffee beans, no *AtNANMT1* homolog could be found in the recently published coffee genome (*Coffea canephora*; http://coffee-genome.org/ [Denoeud et al., 2014]). It should be noted that *NANMT* is a single-copy gene in the sequenced genomes analyzed in this study, except for in soybean, where two copies of the *NANMT* gene were found (Fig. 6A).

We next conducted enzymatic assays with NANMT-like proteins from 10 representative plant species, selected based on the phylogenetic tree in Figure 6A (Matsui et al., 2007; Ashihara et al., 2012). All of the NANMT-like proteins from seed plants had high catalytic efficiency toward NA, with the exception of the NANMT-like protein from *Amborella trichopoda*, a basal angiosperm plant (Fig. 6B; Table I). Interestingly, AtCOMT also showed weak NA *N*-methylation activity (~1.6% of COMT activity toward caffealdehyde; Fig. 6B; Table II). Among the 13 OMTs from basal land plants that we assayed, only Ppa12g019400, Smo438615, and Smo227179 showed NA *N*-methylation activity, and this activity was extremely weak (Fig. 6C; Table II). Ppa12g019400 and Smo438615, like AtCOMT, showed much higher phenylpropanoid methylation activity than NA *N*-methylation activity (Table II; Supplemental Fig. S8). However, Smo227179 showed specificity for NA; it showed no activity toward phenylpropanoid substrates (Table II).

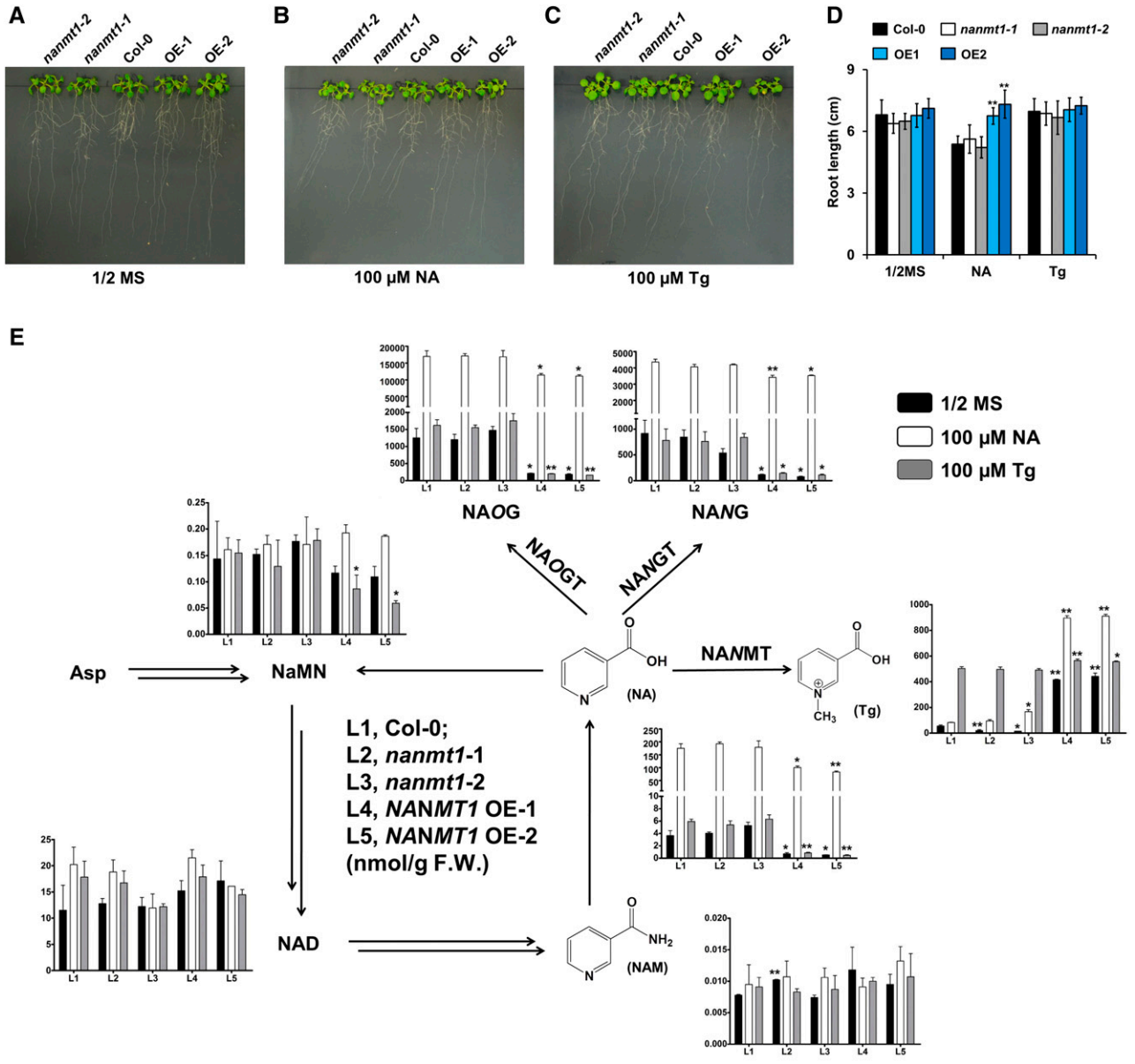

Figure 5. Root growth and chemical analysis of Col-0, *nanmt1* mutants, and *At*NA*NMT1* OE lines exposed to NA and Tg. A to C, Four-day-old seedlings, with 10-mm roots, of Col-0, *nanmt1* mutants, and *At*NA*NMT1* OE lines were transferred from 1/2 MS plates to plates supplemented with 100 μM NA or Tg and grown for 7 additional days. D, Root growth of seedlings grown under 100 μM NA or Tg treatment. Data are presented as means ± SD of four independent experiments (three seedlings of each line were used in one experiment). Asterisks indicate significant differences from Col-0 plants in the same treatment: **, $P < 0.01$ (two-tailed Student's *t* test). E, Chemical analysis of the seedlings of *At*NA*NMT1* transgenic plants under various growth conditions (1/2 MS, NA treatment, and Tg treatment). Bars show means ± SD ($n = 4$). Asterisks indicate significant differences from wild-type plants: *, $P < 0.05$ and **, $P < 0.01$ (two-tailed Student's *t* test). F.W., Fresh weight.

Homology Modeling of NA*N*MT

Multiple sequence alignment revealed that NA*N*MTs contain all of the signature motifs that are conserved among OMT enzymes (Supplemental Fig. S9). To further explore structure-function relationships among the various NA*N*MT proteins, an AtNA*N*MT1 structural model was generated based on the published crystal structures of COMTs from perennial ryegrass (*Lolium perenne*) and alfalfa (*Medicago sativa*; Zubieta et al., 2002; Louie et al., 2010). Structural analysis suggested that there is one catalytic residue, Thr-264, and three substrate-binding residues, Asn-21, Tyr-120, and His-124, in AtNA*N*MT1 (Fig. 7A). The structure of the AtNA*N*MT1 protein docked with SAH and NA also suggested that the carboxyl group (negatively charged)

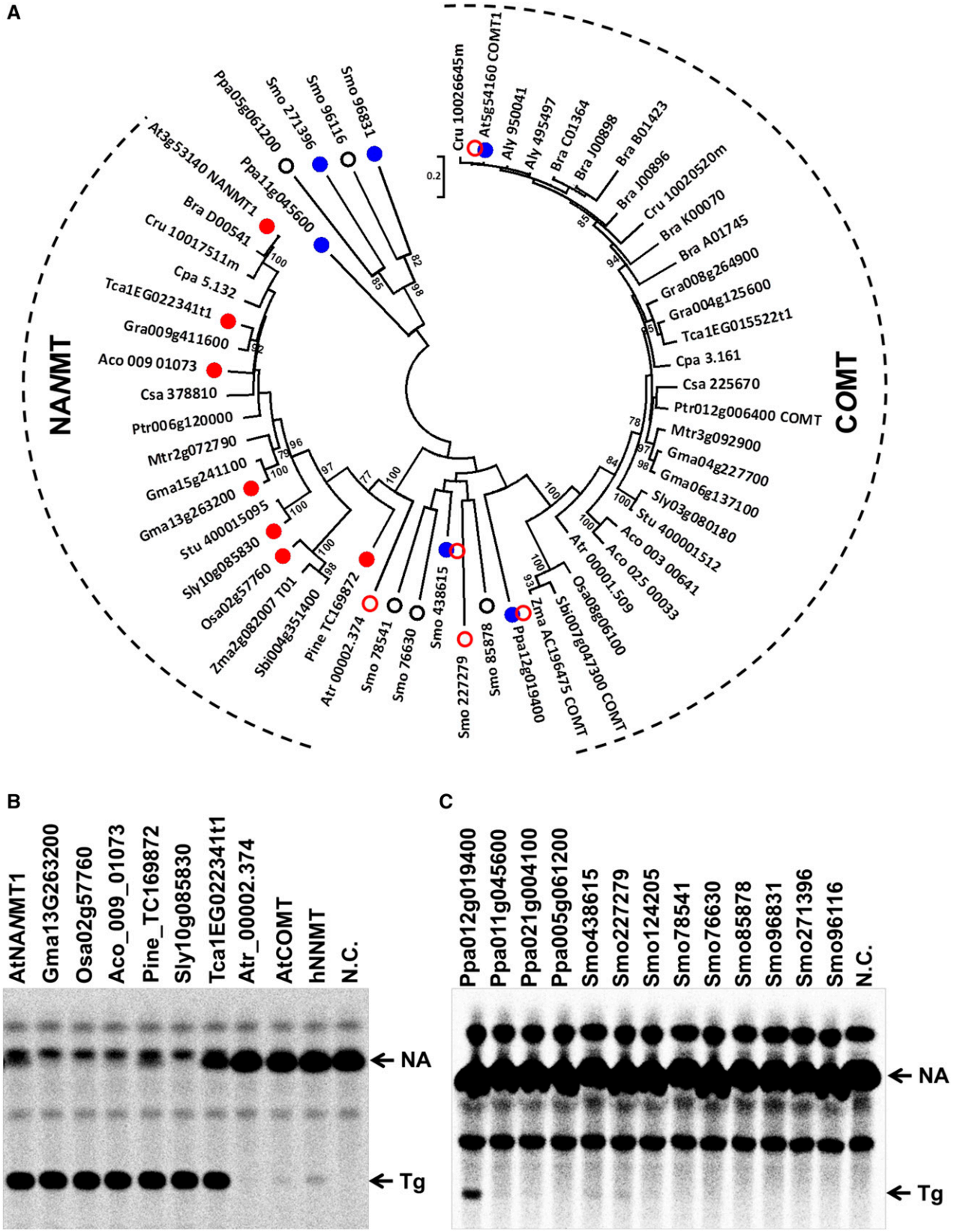

Figure 6. Phylogenetic analysis and biochemical characterization of NA*N*MT-like proteins from diverse land plant taxa. A, Phylogenetic tree of AtNA*N*MT1 and AtCOMT1 (encoded by *At5g54160*) and their homologs from different plant lineages. The

Table II. *Relative activities (%) of plant NANMT and COMT proteins toward NA and phenylpropanoids*
N.D., Not detectable.

Enzyme	NA	Caffeyl Alcohol	Caffealdehyde	Caffeic Acid
AtNA*N*MT1	100[a]	N.D.	N.D.	N.D.
AtCOMT	1.66 ± 0.61[b]	80.84 ± 39.19	104.59 ± 44.32	87.84 ± 35.10
Smo438615	0.52 ± 0.16[b]	84.67 ± 49.96	98.38 ± 44.59	1.96 ± 0.54
Gm13G263200	103.98 ± 5.78	N.D.	N.D.	N.D.
Os02g57760	99.98 ± 10.28	N.D.	N.D.	N.D.
Aco_009_01073	99.23 ± 8.05	N.D.	N.D.	N.D.
PineTC169872	99.71 ± 2.04	N.D.	N.D.	N.D.
Sly10g085830	103.05 ± 13.09	N.D.	N.D.	N.D.
Tca1EG022341t1	79.97 ± 3.70	N.D.	N.D.	N.D.
Atr_00002.374	2.39 ± 0.28	N.D.	N.D.	N.D.
Ppa012g019400	2.90 ± 0.01[b]	74.94 ± 25.19	93.32 ± 16.04	100.29 ± 14.84
Ppa011g045600	N.D.	N.D.	22.61 ± 14.66	46.67 ± 21.54
Ppa021g004100	N.D.	N.D.	N.D.	N.D.
Ppa005g061200	N.D.	N.D.	N.D.	N.D.
Smo227279	0.41 ± 0.00[b]	N.D.	N.D.	N.D.
Smo124205	N.D.	N.D.	18.00 ± 9.25	19.28 ± 11.99
Smo78541	N.D.	N.D.	N.D.	N.D.
Smo76630	N.D.	N.D.	N.D.	N.D.
Smo85878	N.D.	N.D.	N.D.	N.D.
Smo96831	N.D.	N.D.	N.D.	0.9 ± 0.59
Smo271396	N.D.	N.D.	N.D.	6.78 ± 1.25
Smo96116	N.D.	N.D.	N.D.	N.D.

[a]The NA*N*MT activity of AtNA*N*MT1 was set as 100%, representing 0.103 pmol min^{-1} μg^{-1} protein.
[b]These assays were carried out using [^{14}C]NA as substrate.

of NA forms a single hydrogen bond interaction with the imidazole group of the side chain of His-124 (positively charged), which is critical for the substrate specificity of AtNA*N*MT1 toward NA. The replacement of the carboxyl group in NA with an amide group in NAM disrupts this hydrogen bond, resulting in the inactivity of NA*N*MTs toward NAM (Supplemental Fig. S10).

To test whether these predicted residues play a critical role in the AtNA*N*MT-catalyzed *N*-methylation of NA, we changed the Asn-21, Tyr-120, His-124, and Thr-264 of AtNA*N*MT1 to the corresponding residues of the AtCOMT protein, and vice versa. The enzymatic assay results showed that the T264N substitution of the AtNA*N*MT1 catalytic site inactivates the enzyme. Of three putative substrate-binding residues, the H124N substitution completely abolishes the NA *N*-methylation activity, whereas the N21S and Y120L substitutions reduce the NA *N*-methylation activity by ~25% and ~65%, respectively (Fig. 7B). None of the mutated AtNA*N*MT1 proteins had COMT activity. All mutated AtCOMT proteins (S25N, L125Y, N129H, and H267T) had no NA*N*MT activity (Fig. 7C).

DISCUSSION

We previously demonstrated that free NA, which is toxic to plant cells, emerged in plant metabolism when the Preiss-Handler NAD salvage pathway was evolved in land plants (Li et al., 2015b). The advantage for land plants of using the Preiss-Handler pathway instead of a two-step NAD salvage pathway remains unclear. Plants have evolved strategies to adapt to the toxicity of NA, which represents an endogenous constraint on plant

Figure 6. (*Continued.*)
proteins with confirmed NA*N*MT and COMT activity are highlighted, respectively, with red circles and blue circles (closed circles, relatively strong activity; open circles, relatively weak activity). Proteins lacking detectable NA*N*MT or COMT activity are marked with black open circles (see B and C). Bootstrap values (based on 500 replicates) > 70% are shown for the corresponding nodes. The scale indicates evolutionary distance in substitutions per site. Species abbreviations are as follows: Aco, *Aquilegia coerulea*; Aly, *Arabidopsis lyrata*; At, *Arabidopsis thaliana*; Atr, *Amborella trichopoda*; Bra, *Brassica rapa*; Cpa, *Carica papaya*; Cru, *Capsella rubella*; Csa, *Cucumis sativus*; Gma, *Glycine max*; Mtr, *Medicago truncatula*; Osa, *Oryza sativa*; Pab, *Picea abies*; Ppa, *Physcomitrella patens*; Ptr, *Populus trichocarpa*; Sbi, *Sorghum bicolor*; Sly, *Solanum lycopersicum*; Smo, *Selaginella moellendorffii*; Stu, *Solanum tuberosum*; Zma, *Zea mays*. B, Radio-TLC analysis of Tg produced by the NA*N*MT candidate proteins from seed plants using [^{14}C]NA and SAM as substrates. AtNA*N*MT1 was used as a positive control. N.C., Negative control, in which no protein was added to the assay. C, Radio-TLC analysis of Tg produced by the NA*N*MT candidate proteins from *P. patens* and *S. moellendorffii* using [^{14}C]NA and SAM as substrates. Note that the assays in this experiment were incubated for 48 h rather than for the 2 h used for the assays in B.

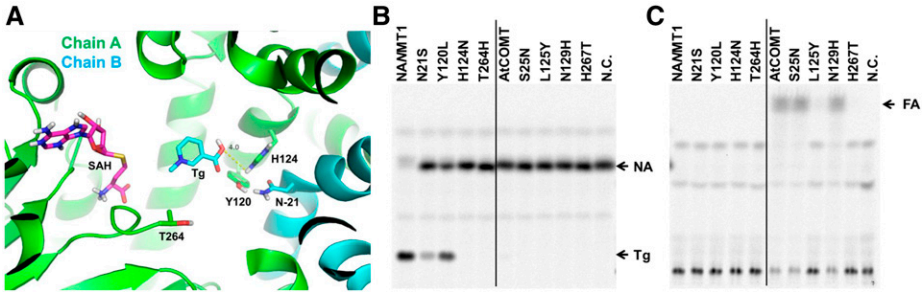

Figure 7. Characterization of key catalytic sites of AtNA*N*MT1. A, Molecular modeling of AtNA*N*MT1. The putative active sites, SAH and Tg, are shown as sticks (cyan, carbon; red, oxygen; blue, nitrogen; yellow, sulfur). B, Radio-TLC analysis of NA*N*MT activity with the purified recombinant proteins using [^{14}C]NA and SAM as substrates. N.C., Negative control, in which no protein was added to the assay. C, Radio-TLC analysis of COMT activity of the purified recombinant proteins using [^{14}C]SAM and caffeic acid as substrates. FA, Ferulic acid.

growth and development. Consistent with this concept, the capacity to make at least one chemical modification to NA (either glycosylation or methylation of the *N*-position or carboxyl group of NA) is present in all tested land plants (Matsui et al., 2007; Ashihara et al., 2012; Li et al., 2015b), including those evaluated in this study. NA glucosylation was demonstrated at the genetic level to function in the detoxification of endogenous NA stress in Brassicaceae plants (Li et al., 2015b). Moreover, in this study, we found that Tg biosynthesis represents a conserved detoxification mechanism for managing free NA, an idea supported by the comparison of root growth of *AtNANMT1* transgenic plants under NA/NAM treatments (Fig. 5). In addition to our findings relating to the detoxification of NA, our results also show that there is an obvious difference in the relationship of NA glucosylation and NA *N*-methylation to NAD homeostasis in Arabidopsis; NA *N*-methylation is clearly involved in the regulation of NAD homeostasis, at least in inflorescence tissue, based on the observation that NAD levels are increased significantly in the *nanmt1* mutants and decreased in the *AtNANMT1* OE lines (Fig. 3). In contrast, NA glucosylation does not influence NAD homeostasis. This phenomenon could be explained by the fact that AtNA*N*MT1 shows much higher efficiency toward NA and SAM than AtNAGTs show toward NA and UDP-Glc (Li et al., 2015b).

Based on our phylogenetic analysis and biochemical characterization of NA*N*MTs and COMTs from various plant species that are positioned at important evolutionary nodes, we hypothesize that NA*N*MT, which has *N*-methylation activity, was derived from the duplication of a *COMT* gene in an ancestral Pteridophytes species. The widespread occurrence of functional COMTs in land plants (from *P. patens* to flowering plants) observed in our study and the discovery of lignin-like compounds in green algae and red algae also support this hypothesis (Delwiche et al., 1989; Martone et al., 2009; Weng et al., 2011). Additionally, all of the COMTs that we tested had weak NA *N*-methylation activity (Table II; Supplemental Fig. S8). Arabidopsis COMT1 is known to be a multifunctional enzyme with activity toward both flavonoids and phenylpropanoids (Nakatsubo et al., 2008; Weng et al., 2011). Recently, the capacity to catalyze the methylation of *N*-acetylserotonin to form melatonin also was assigned to the Arabidopsis COMT1 protein (Byeon et al., 2014). These observations are consistent with the theory that catalytic promiscuity serves as the starting point for the acquisition of new enzymatic functions; a newly emerged NA*N*MT enzyme likely adopted one of the minor activities of the ancestral COMT (Aharoni et al., 2005; Weng, 2014). Based on our data, we can deduce the phylogeny of NA*N*MT enzymes; the minor NA *N*-methylation activity was acquired in a COMT duplicated copy in the Bryophytes (Ppa012g019400 in *P. patens*) after the basal land plant recruited the Preiss-Handler NAD salvage pathway; then, a COMT copy evolved into an NA-specific protein in Pteridophytes (Smo227279 in *S. moellendorffii*). Then, the primitive NA*N*MT was evolved into a high-efficiency NA *N*-methylation enzyme and was retained in higher plants. During this process, several amino acids (such as His-124 and Thr-264 in the AtNA*N*MT1 protein) were likely under positive selection. The weak NA*N*MT activity of the AtCOMT1 protein and the high expression level of *AtCOMT1* are likely responsible for the low but detectable levels of Tg in *nanmt1* mutant plants (Supplemental Fig. S11). In addition to the NA*N*MT1 identified in this study, there are 12 additional COMT-like proteins in the Arabidopsis genome; these promise to be useful resources for the discovery of other novel methyltransferase activities (Weng et al., 2011).

Given the conservation of *NANMT* in land plants, it is surprising that there appear to be no *AtNANMT1* homologs in the coffee genome, as Tg accounts for more than 1% of the dry matter in coffee beans (Allred et al., 2009). However, two SABATH proteins, which share more than 80% identity with coffee caffeine synthase, were identified as NA*N*MT enzymes in coffee (Mizuno et al., 2014). All three enzymes belong to the SABATH gene family, which is distantly related to the *COMT* and *NANMT* gene families. It is reasonable to deduce that the coffee *NANMT* genes evolved more than once (a case of convergent evolution) from the expansion of the

SABATH gene family (23 members in the coffee genome) and that the *AtNANMT1* homolog was lost during the evolution of coffee (Pichersky and Lewinsohn, 2011; Denoeud et al., 2014). However, it is not clear whether the gain of NA *N*-methylation activity from a *SABATH* gene predates the loss of the *NANMT1* homolog or vice versa, although the former is more likely because of the toxicity of NA. A comprehensive analysis of related enzymes in coffee and related wild relative species will likely be required to answer this question.

In conclusion, we have identified and biochemically characterized a unique group of NANMTs from land plants. These enzymes are involved in NA detoxification and function to fine-tune NAD homeostasis. The residues that are critical for NA *N*-methylation activity were determined using OMT structural modeling and mutagenesis studies. Our phylogenetic analysis suggests that the recruitment of NA *N*-methylation activity might have resulted from the duplication of plant *COMT* genes before the Pteridophytes diverged from the Bryophytes. Finally, we should emphasize that the NA detoxification conferred by NANMT activity might have facilitated the retention of the Preiss-Handler pathway in land plants.

MATERIALS AND METHODS

Plant Materials and Chemicals

The wild-type (ecotype Col-0) and transgenic Arabidopsis (*Arabidopsis thaliana*) lines used in this study were grown on soil at 22°C under a 16-h-light/8-h-dark cycle. *Chlamydomonas reinhardtii* (strain cc-400 cw15 mt+) was obtained from the *Chlamydomonas* Genetic Center (http://www.chlamycollection.org). All chemicals used in this study were purchased from Sigma-Aldrich except for the radiolabeled compounds [carboxyl-^{14}C]NAM and [carboxyl-^{14}C]NA (55 mCi mmol^{-1}), which were purchased from American Radiolabeled Chemicals, and [^{14}C]SAM (48.8 mCi mmol^{-1}), which was purchased from PerkinElmer.

MT Gene-NANMT Activity Correlation Analysis

Pearson's correlation analysis (two tailed) was performed using SPSS software (version 19.0; IBM Software). Transcript expression data for 289 putative methyltransferase genes was bulk downloaded from ATTEDII (version 8.0; http://atted.jp/). Levels of [^{14}C]Tg accumulation (the indicator of NANMT activity) were determined directly from radio-TLC images using ImageJ 1.38e software (downloaded from the U.S. National Institutes of Health; http://rsb.info.nih.gov/ij/). To simplify the analysis procedure, all transcript and metabolite accumulation data were transformed into relative format, meaning that the value of the largest data point was set as 1 (for details, see Supplemental Data Set S1).

AtNANMT1 Expression, Purification, and Enzyme Assays

To generate *N*-terminally MBP-tagged NANMT, the ORFs of putative *NANMT* genes from different species were PCR amplified if the plant materials were available, and the appropriate digestion sites were incorporated into the primers used for PCR cloning. Additionally, 13 putative *NANMT* genes (*Aco_009_01073*, *Atr_00002.374*, *PineTC169872*, *Sly10g085830*, *Tca1EG022341t1*, *Ppa005G061200*, *Ppa021G004100*, *Smo78541*, *Smo76630*, *Smo85878*, *Smo96831*, *Smo271396*, and *Smo96116*; for detailed sequence information, see Supplemental Data Set S2) and the human *NNMT* gene, including introduced digestion sites, were synthesized by GenScript because fresh material was unavailable. After confirming the identity of the amplified products by sequencing, the PCR fragments were digested and ligated into the pMAL-c2X vector (New England Biolabs). The resulting MBP-tag fusion proteins were purified using affinity chromatography on an amylase resin following the manufacturer's instructions. Quantification and evaluation of the relative purity of the recombinant proteins were conducted via SDS-PAGE using BSA as a standard. NANMT assays were performed in a Tris-HCl buffer (50 mM, pH 7.5) with appropriate amounts of SAM and [^{14}C]NA (diluted with cold NA if necessary). The reactions with proteins from basal land plants were incubated at 28°C for 48 h. All other recombinant proteins were incubated at 28°C for 2 h. The ^{14}C-labeled enzymatic products and the standard were spotted on silica TLC plates and developed with an *n*-butanol:HOAc:water system (2:1:1). The radio spots on the TLC plate were measured using a radio scanner (Wang and Pichersky, 2007; Li et al., 2015b).

To obtain pure [carboxyl-^{14}C]Tg, a reaction including 400 μM SAM, 100 μM [carboxyl-^{14}C]NA, and an appropriate amount of purified AtNANMT1 protein was incubated at 28°C for 48 h. The 100% conversion ratio from [carboxyl-^{14}C]NA to [carboxyl-^{14}C]Tg was verified with the above-mentioned TLC method.

Quantitative PCR Analysis and GUS Staining

RNA extraction, reverse transcription reaction, quantitative PCR, and *Pro$_{NANMT1}$:GUS* (the *Pro$_{NANMT1}$* is approximately 0.5 kb in length) experiments were performed as described previously (Li et al., 2015a, 2015b). Detailed primer information see Supplemental Data Set S4.

Subcellular Localization of AtNANMT1

Subcellular localization, including the construction of the AtNANMT1-GFP fusion protein (pJIT163-hGFP vector), preparation of Arabidopsis leaf protoplasts, protoplast transformation, and image collection using a laser scanning confocal microscope, was performed as described previously (Xu et al., 2013). For detailed primer information, see Supplemental Data Set S4.

Liquid Chromatography-Mass Spectrometry Analysis

The endogenous levels of NA, Tg, and the NAD-related chemicals were determined with an ultra-performance liquid chromatography-tandem mass spectrometry analytical platform consisting of an Agilent 1290 Infinity liquid chromatography pump and a 6495 triple quadrupole mass spectrometer (Agilent), following the protocol described in our previous study (Li et al., 2015b).

Phylogenetic Analysis

The sequences of AtNANMT1 and AtCOMT1 (encoded by *At5g54160*) and MT proteins with high identity (greater than 40%) to AtNANMT1 and AtCOMT1 from other plant species were extracted from TAIR (http://www.arabidopsis.org) and Phytozome 10.3 databases (http://www.phytozome.net; for detailed sequence information, see Supplemental Data Set S3). A maximum likelihood tree was constructed using MEGA6.0 software (Tamura et al., 2013).

Homology Modeling and Docking

The AtNANMT1 sequence was used as a query in a BLAST search against the Protein Data Bank (http://www.rcsb.org/pdb/), and six proteins that share 35% to 60% identity with AtNANMT1 were selected (Protein Data Bank identifiers 1FP1, 1KYW, 3P9K, 3TKY, 4PGH, and 5CVJ). Based on the six crystal structure models, we used the MODELER software to construct the protein models with SAH as a cofactor and NA as the substrate (Sali and Blundell, 1993). After model building, the Gromacs version 5.1.2 (www.gromacs.org) program with the CHARMM36 force field was used for local energy minimization. The AtNANMT1 model was set in the center of a water box solvated with simple point charge (SPC)-type water molecules. Additionally, Na^+ and Cl^- ions were placed randomly in the simulation system to neutralize it and to set the NaCl concentration to 0.1 M. Finally, the overall quality factor of the modeled structure was assessed using the ERRAT and PROCHECK programs (Colovos and Yeates, 1993; Laskowski et al., 1993). For protein-ligand docking, simulations were performed using the AutoDockTools and AutoDock Vina, with the protein as a receptor and Tg as a ligand (Morris et al., 2009; Trott and Olson, 2010), and the top hit was chosen for subsequent biochemical validation. PyMOL (version 1.3) was used for protein model visualization.

Supplemental Data

The following supplemental materials are available.

Supplemental Figure S1. *P. patens* and *S. moellendorffii* plants and the tissues analyzed in this study.

Supplemental Figure S2. Assays evaluating the influence of pH and metal ions on the relative activity of AtNANMT1 ($n = 3$).

Supplemental Figure S3. Characterization of *AtNANMT1* transgenic plants.

Supplemental Figure S4. Transcript analysis of NAD-related genes in *NANMT1* transgenic plants.

Supplemental Figure S5. Chemical characterization of developing seeds (from 9- to 10-week-old siliques) of *AtNANMT1* transgenic plants.

Supplemental Figure S6. Phenotypic analyses of *AtNANMT1* transgenic plants.

Supplemental Figure S7. Metabolic fate of [carboxyl-^{14}C]Tg in different Arabidopsis tissues.

Supplemental Figure S8. Substrate specificity of AtNANMT, AtCOMT, Smo438615, and Ppa012g019400 determined using [^{14}C]SAM (40 μM) and cold NA or phenylpropanoids (100 μM) as cosubstrates.

Supplemental Figure S9. Multiple sequence alignment of NANMTs and COMTs from various plant lineages.

Supplemental Figure S10. Radio-TLC analysis of *N*-methylnicotinamide generated by the NANMT candidate proteins from representative seed plants using [^{14}C]NAM and SAM as substrates.

Supplemental Figure S11. Tissue specificity of *AtCOMT1* and *AtNANMT1* expression.

Supplemental Data Set S1. Pearson correlation analysis of NANMT activity ([^{14}C]Tg signal) and expression levels of Arabidopsis methyltransferase genes.

Supplemental Data Set S2. Synthesized genes used in this study.

Supplemental Data Set S3. COMT and NANMT sequences included in phylogenic analysis.

Supplemental Data Set S4. Primers used in this study.

ACKNOWLEDGMENTS

We thank Dr. Guanghong Chi (Chinese Academy of Sciences) for efforts at the early stage of this project, Dr. Aixia Cheng (Shandong University) for providing chemicals for the COMT assays, Dr. Clint Chapple (Purdue University) for providing four COMT-like cDNA clones from *S. moellendorffii*, and Dr. Yikun He (Capital Normal University) for providing the *P. patens* materials.

Received April 13, 2017; accepted May 18, 2017; published May 22, 2017.

LITERATURE CITED

Aharoni A, Gaidukov L, Khersonsky O, McQ Gould S, Roodveldt C, Tawfik DS (2005) The 'evolvability' of promiscuous protein functions. Nat Genet **37:** 73–76

Aksoy S, Szumlanski CL, Weinshilboum RM (1994) Human liver nicotinamide *N*-methyltransferase: cDNA cloning, expression, and biochemical characterization. J Biol Chem **269:** 14835–14840

Allred KF, Yackley KM, Vanamala J, Allred CD (2009) Trigonelline is a novel phytoestrogen in coffee beans. J Nutr **139:** 1833–1838

Ashihara H, Yin Y, Katahira R, Watanabe S, Mimura T, Sasamoto H (2012) Comparison of the formation of nicotinic acid conjugates in leaves of different plant species. Plant Physiol Biochem **60:** 190–195

Byeon Y, Lee HY, Lee K, Back K (2014) Caffeic acid O-methyltransferase is involved in the synthesis of melatonin by methylating N-acetylserotonin in Arabidopsis. J Pineal Res **57:** 219–227

Colovos C, Yeates TO (1993) Verification of protein structures: patterns of nonbonded atomic interactions. Protein Sci **2:** 1511–1519

De Block M, Van Lijsebettens M (2011) Energy efficiency and energy homeostasis as genetic and epigenetic components of plant performance and crop productivity. Curr Opin Plant Biol **14:** 275–282

Delwiche CF, Graham LE, Thomson N (1989) Lignin-like compounds and sporopollenin coleochaete, an algal model for land plant ancestry. Science **245:** 399–401

Denoeud F, Carretero-Paulet L, Dereeper A, Droc G, Guyot R, Pietrella M, Zheng C, Alberti A, Anthony F, Aprea G, et al (2014) The coffee genome provides insight into the convergent evolution of caffeine biosynthesis. Science **345:** 1181–1184

Evans LS, Almeida MS, Lynn DG, Nakanishi K (1979) Chemical characterization of a hormone that promotes cell arrest in g2 in complex tissues. Science **203:** 1122–1123

Gang DR, Lavid N, Zubieta C, Chen F, Beuerle T, Lewinsohn E, Noel JP, Pichersky E (2002) Characterization of phenylpropene *O*-methyltransferases from sweet basil: facile change of substrate specificity and convergent evolution within a plant *O*-methyltransferase family. Plant Cell **14:** 505–519

Goujon T, Sibout R, Pollet B, Maba B, Nussaume L, Bechtold N, Lu F, Ralph J, Mila I, Barrière Y, et al (2003) A new *Arabidopsis thaliana* mutant deficient in the expression of O-methyltransferase impacts lignins and sinapoyl esters. Plant Mol Biol **51:** 973–989

Katoh A, Uenohara K, Akita M, Hashimoto T (2006) Early steps in the biosynthesis of NAD in Arabidopsis start with aspartate and occur in the plastid. Plant Physiol **141:** 851–857

Laskowski RA, Moss DS, Thornton JM (1993) Main-chain bond lengths and bond angles in protein structures. J Mol Biol **231:** 1049–1067

Li H, Ban Z, Qin H, Ma L, King AJ, Wang G (2015a) A heteromeric membrane-bound prenyltransferase complex from hop catalyzes three sequential aromatic prenylations in the bitter acid pathway. Plant Physiol **167:** 650–659

Li W, Zhang F, Chang Y, Zhao T, Schranz ME, Wang G (2015b) Nicotinate *O*-glucosylation is an evolutionarily metabolic trait important for seed germination under stress conditions in *Arabidopsis thaliana*. Plant Cell **27:** 1907–1924

Liscombe DK, Louie GV, Noel JP (2012) Architectures, mechanisms and molecular evolution of natural product methyltransferases. Nat Prod Rep **29:** 1238–1250

Louie GV, Bowman ME, Tu Y, Mouradov A, Spangenberg G, Noel JP (2010) Structure-function analyses of a caffeic acid *O*-methyltransferase from perennial ryegrass reveal the molecular basis for substrate preference. Plant Cell **22:** 4114–4127

Martin JL, McMillan FM (2002) SAM (dependent) I AM: the S-adenosylmethionine-dependent methyltransferase fold. Curr Opin Struct Biol **12:** 783–793

Martone PT, Estevez JM, Lu F, Ruel K, Denny MW, Somerville C, Ralph J (2009) Discovery of lignin in seaweed reveals convergent evolution of cell-wall architecture. Curr Biol **19:** 169–175

Matsui A, Yin Y, Yamanaka K, Iwasaki M, Ashihara H (2007) Metabolic fate of nicotinamide in higher plants. Physiol Plant **131:** 191–200

McCarthy AA, McCarthy JG (2007) The structure of two *N*-methyltransferases from the caffeine biosynthetic pathway. Plant Physiol **144:** 879–889

Minorsky PV (2002) Trigonelline: a diverse regulator in plants. Plant Physiol **128:** 7–8

Mizuno K, Matsuzaki M, Kanazawa S, Tokiwano T, Yoshizawa Y, Kato M (2014) Conversion of nicotinic acid to trigonelline is catalyzed by *N*-methyltransferase belonged to motif B′ methyltransferase family in *Coffea arabica*. Biochem Biophys Res Commun **452:** 1060–1066

Morris GM, Huey R, Lindstrom W, Sanner MF, Belew RK, Goodsell DS, Olson AJ (2009) AutoDock4 and AutoDockTools4: automated docking with selective receptor flexibility. J Comput Chem **30:** 2785–2791

Nakatsubo T, Kitamura Y, Sakakibara N, Mizutani M, Hattori T, Sakurai N, Shibata D, Suzuki S, Umezawa T (2008) *At5g54160* gene encodes *Arabidopsis thaliana* 5-hydroxyconiferaldehyde *O*-methyltransferase. J Wood Sci **54:** 312–317

Noctor G, Queval G, Gakière B (2006) NAD(P) synthesis and pyridine nucleotide cycling in plants and their potential importance in stress conditions. J Exp Bot **57:** 1603–1620

Peng Y, Sartini D, Pozzi V, Wilk D, Emanuelli M, Yee VC (2011) Structural basis of substrate recognition in human nicotinamide *N*-methyltransferase. Biochemistry **50:** 7800–7808

Pichersky E, Lewinsohn E (2011) Convergent evolution in plant specialized metabolism. Annu Rev Plant Biol **62:** 549–566

Preiss J, Handler P (1958a) Biosynthesis of diphosphopyridine nucleotide. I. Identification of intermediates. J Biol Chem **233:** 488–492

Preiss J, Handler P (1958b) Biosynthesis of diphosphopyridine nucleotide. II. Enzymatic aspects. J Biol Chem **233:** 493–500

Rongvaux A, Andris F, Van Gool F, Leo O (2003) Reconstructing eukaryotic NAD metabolism. BioEssays **25:** 683–690

Sali A, Blundell TL (1993) Comparative protein modelling by satisfaction of spatial restraints. J Mol Biol **234:** 779–815

Shimizu MM, Mazzafera P (2000) A role for trigonelline during imbibition and germination of coffee seeds. Plant Biol **2:** 605–611

Tamura K, Stecher G, Peterson D, Filipski A, Kumar S (2013) MEGA6: molecular evolutionary genetics analysis version 6.0. Mol Biol Evol **30:** 2725–2729

Trott O, Olson AJ (2010) AutoDock Vina: improving the speed and accuracy of docking with a new scoring function, efficient optimization, and multithreading. J Comput Chem **31:** 455–461

Upmeier B, Gross W, Köster S, Barz W (1988) Purification and properties of S-adenosyl-L-methionine:nicotinic acid-N-methyltransferase from cell suspension cultures of Glycine max L. Arch Biochem Biophys **262:** 445–454

van Dijk AE, Olthof MR, Meeuse JC, Seebus E, Heine RJ, van Dam RM (2009) Acute effects of decaffeinated coffee and the major coffee components chlorogenic acid and trigonelline on glucose tolerance. Diabetes Care **32:** 1023–1025

Wang G, Pichersky E (2007) Nicotinamidase participates in the salvage pathway of NAD biosynthesis in Arabidopsis. Plant J **49:** 1020–1029

Weng JK (2014) The evolutionary paths towards complexity: a metabolic perspective. New Phytol **201:** 1141–1149

Weng JK, Akiyama T, Ralph J, Chapple C (2011) Independent recruitment of an O-methyltransferase for syringyl lignin biosynthesis in *Selaginella moellendorffii*. Plant Cell **23:** 2708–2724

Xu H, Zhang F, Liu B, Huhman DV, Sumner LW, Dixon RA, Wang G (2013) Characterization of the formation of branched short-chain fatty acid:CoAs for bitter acid biosynthesis in hop glandular trichomes. Mol Plant **6:** 1301–1317

Yang Y, Varbanova M, Ross J, Wang G, Cortes D, Fridman E, Shulaev V, Noel JP, Pichersky E (2006a) Methylation and demethylation of plant signaling molecules. *In* JT Romeos, ed, Recent Advances in Phytochemistry. Elsevier Science, Oxford, pp 253–270

Yang Y, Yuan JS, Ross J, Noel JP, Pichersky E, Chen F (2006b) An *Arabidopsis thaliana* methyltransferase capable of methylating farnesoic acid. Arch Biochem Biophys **448:** 123–132

Zheng XQ, Hayashibe E, Ashihara H (2005) Changes in trigonelline (*N*-methylnicotinic acid) content and nicotinic acid metabolism during germination of mungbean (*Phaseolus aureus*) seeds. J Exp Bot **56:** 1615–1623

Zhou J, Chan L, Zhou S (2012) Trigonelline: a plant alkaloid with therapeutic potential for diabetes and central nervous system disease. Curr Med Chem **19:** 3523–3531

Zubieta C, He XZ, Dixon RA, Noel JP (2001) Structures of two natural product methyltransferases reveal the basis for substrate specificity in plant O-methyltransferases. Nat Struct Biol **8:** 271–279

Zubieta C, Kota P, Ferrer JL, Dixon RA, Noel JP (2002) Structural basis for the modulation of lignin monomer methylation by caffeic acid/5-hydroxyferulic acid 3/5-*O*-methyltransferase. Plant Cell **14:** 1265–1277